Since January 2020 Elsevier has created a COVID-19 resource centre with free information in English and Mandarin on the novel coronavirus COVID-19. The COVID-19 resource centre is hosted on Elsevier Connect, the company's public news and information website.

Microchemical Journal 166 (2021) 106249

Contents lists available at ScienceDirect

Microchemical Journal

journal homepage: www.elsevier.com/locate/microc

A paper-based electrochemical sensor for H_2O_2 detection in aerosol phase: Measure of H_2O_2 nebulized by a reconverted ultrasonic aroma diffuser as a case of study

Luca Fiore [a], Vincenzo Mazzaracchio [a], Pierluca Galloni [a,b], Federica Sabuzi [a,b], Silvia Pezzola [b], Giorgia Matteucci [b], Danila Moscone [a], Fabiana Arduini [a,c,*]

[a] Department of Chemical Science and Technologies, University of Rome Tor Vergata, Via della Ricerca Scientifica 1, Rome 00133, Italy
[b] BT-INNOVACHEM, Via della Ricerca Scientifica 1, Rome, 00133, Italy
[c] SENSE4MED, Via Renato Rascel 30, Rome 00128, Italy

ARTICLE INFO

Keywords:
Screen-printed electrodes
Carbon black
Prussian-blue nanoparticles
Amperometry

ABSTRACT

The outbreak of COVID-19 is caused by high contagiousness and rapid spread of SARS-CoV-2 virus between people when an infected person is in close contact with another one. In this overall scenario, the disinfection processes have been largely improved. For instance, some countries have approved no-touch technologies by vaporizing disinfectants such as hydrogen peroxide, with the overriding goal to boost the safety of the places. In the era of sustainability, we designed an electrochemical paper-based device for the assessment of hydrogen peroxide nebulized by a cost-effective ultrasonic aroma diffuser. The paper-based sensor was fabricated by modifying *via* drop-casting a filter paper-based screen-printed electrode with a dispersion of carbon black-Prussian Blue nanocomposite, to assess the detection of hydrogen peroxide at −0.05 V vs Ag/AgCl. The use of paper-based modified screen-printed electrode loaded with phosphate buffer allowed for monitoring the concentration of hydrogen peroxide in aerosol, without any additional sampling instrument to capture the nebulized solution of hydrogen peroxide at a concentration up to 7% w/w. Hydrogen peroxide, a reconverted ultrasonic aroma diffuser, and the paper-based electrochemical sensor assisted by smartphone have demonstrated how different low-cost technologies are able to supply an useful and cost-effective solution for disinfection procedures.

1. Introduction

The outbreak of SARS-CoV-2 is having a large impact on the health of citizens at a worldwide level as well as on the healthcare management and economy in each country that must face this huge pandemic event. The easy spread of SARS-CoV-2 and its persistence are some of the key issues of the prevalence and contagiousness of COVID-19. The principal way by which people are infected is through exposure to mucosalivary droplets formed during breathing, speaking, coughing, and sneezing. Among mucosalivary droplets, larger droplets rapidly fall out, while smaller droplets remain suspended for a longer time and they are able to travel through air currents [1]. Indeed, as reported by L. Bourouiba, the mucosalivary droplets are primarily made of a multiphase turbulent gas cloud, able to avoid evaporation for a much longer time in respect to isolated droplets, with a probable lifetime enlarged by a factor of up to 1000, from a fraction of a second to minutes, thus augmenting the presence of droplets in the air [2].

The other key issue is the persistence on the environmental surfaces; indeed SARS-CoV-2 remains on clothes up to one day, on banknotes up to two days, on stainless steel, plastic and the inner layer of the mask up to four days, and on the outer layer of the mask up to seven days [3], demonstrating the need of disinfection to avoid the spread of SARS-CoV-2 by contact. SARS-CoV-2 survives in a wide range of pH values and ambient temperatures but, fortunately, it is vulnerable to heat and standard disinfection methods such as the one based on chlorine-based product, adopted as reported by WHO [4]. In addition, some countries have approved no-touch technologies by vaporizing disinfectants such as hydrogen peroxide, using customized instrumentations [4,5]. Hydrogen peroxide is a compound characterized by high oxidant properties, being able to produce hydroxyl radicals that attack DNA,

* Corresponding author at: Department of Chemical Science and Technologies, University of Rome Tor Vergata, Via della Ricerca Scientifica 1, Rome 00133, Italy.
E-mail address: fabiana.arduini@uniroma2.it (F. Arduini).

https://doi.org/10.1016/j.microc.2021.106249
Received 3 February 2021; Received in revised form 24 March 2021; Accepted 1 April 2021
Available online 5 April 2021

membrane lipids, and other essential cell components. SARS-CoV-2 is an enveloped virus, thus characterized by a breakable outer lipid envelope that renders it more vulnerable to disinfectants compared with non-enveloped viruses, such as rotavirus and poliovirus. The major types of hydrogen peroxide room disinfection devices are based on aerosolized hydrogen peroxide systems (e.g. GLOSAIR; Advanced Sterilization Products, Irvine, CA) or hydrogen peroxide vapor systems (e.g. Bioquell, Andover, Hampshire, UK) using hydrogen peroxide in the range of 5–15 % w/w [5]. As in the case of the insufficient amount of personal protective equipment at the start of the COVID-19 outbreak, when several industries have reset their production chain to urgently supply them, the commercially available ultrasonic aroma diffuser with very low cost (lower than 20 €) can be reconverted for the disinfection of rooms at home or in offices using hydrogen peroxide as a disinfectant. However, one of the parameters to be controlled relies on the amount of hydrogen peroxide spread by the diffuser, being the hydrogen peroxide an unstable compound. Thus, a cost-effective sensing system is needed to assess the hydrogen peroxide concentration and to customize the correct disinfection process, avoiding excessive use of the disinfectant.

The use of paper in the development of electrochemical devices has attracted huge attention by scientific community, due to its low cost and unexpected and unprecedented features, being able to create microfluidic patterns without expensive instrumentation and the requirement of external pumps [6,7]. In addition, the porosity of the paper has been used to load the reagents, delivering reagent-free devices [8,9]. Furthermore, the porosity of the paper has been also recently exploited to detect analytes in the gas phase without any sampling system, as demonstrated by our group in the case of a wearable sensor for mustard agent detection [10] and by Dincer's group for the hydrogen peroxide monitoring in breath [11]. Indeed, the porous structure of paper allows for loading the reagents, and the aerosol is sufficient to wet the cellulose network, allowing for the measure in the thin film layer of the solution within the cellulose network. In our previous work, we used an origami system to load reagents, namely enzyme and substrate, waiting that the two layers of the paper became wet. After, the two layers of paper were put in close contact and exposed to the mustard agent aerosol, demonstrating the capability to detect the aerosol by using paper-based devices without any additional sampling system [10].

Herein, we demonstrated for the first time that the modification via drop-casting with nanomaterials is not relegated to office paper-based sensors, but it is applicable also in the case of filter paper-based sensors, allowing for a cost-effective mass-production of sensors. In addition, we reported a novel smartphone based electrochemical device with a paper-based sensor for the measure of hydrogen peroxide aerosol produced by an ultrasonic aroma reconverted diffuser, with the aim to boost a cost-effective, reliable, and controlled room disinfection system.

2. Experimental section

2.1. Reagents and equipment

Potassium chloride, phosphoric acid, hydrogen peroxide 30% (w/w), N,N-dimethylformamide were purchased from Sigma Aldrich (St. Louis, MO, USA). Carbon Black N220 was kindly gifted by Cabot, Ravenna, Italy. Carbon black/Prussian blue nanoparticles (CB/PBNPs) powder was synthesized by using $K_3Fe(CN)_6$ and HCl obtained from Sigma, and $FeCl_3$ from Fluka. Mueller Hinton agar plates (Liofilchem®, Italy) for cultivating bacteria and Sabouraud dextrose agar plates (Liofilchem®, Italy) for fungi and yeasts. Micrographs of the bare screen-printed electrode and the screen-printed electrode modified with nanocomposite constituted of carbon black and Prussian Blue nanoparticles were acquired by means of electron microscopy FEI Quanta 400. A ColorQube 8580 Xerox printer (Xerox Corporation, USA) was used to print the wax patterns. The paper-based electrodes were produced by SENSE4MED Company (Rome, Italy) with 245 DEK (Weymouth, UK) serigraphic printer using graphite-based ink (Electrodag 421) for the printing of tracks, counter, and working electrode, while silver/silver chloride ink (Electrodag 4038 SS) was used for the printing of reference electrode. Cyclic voltammetry and chronoamperometry were carried out using a portable potentiostat, Sensit Smart (PalmSens, Netherlands), in connection with a smartphone.

2.2. Paper-based screen-printed electrode preparation

Filter paper-based screen-printed electrodes (SPEs) unmodified and modified with CB/PBNPs nanocomposite 0.3% w/w were supplied by SENSE4MED (Rome, Italy). The whole sensor is characterized by a dimension of 28 mm length × 12 mm width, while the diameter of working electrode is equal to 4 mm. For modification *via* drop-casting of filter paper-based SPEs, a 2 μL-drop of CB/PBNPs dispersion 0.06 mg/mL was cast onto the working electrode of the SPE. The CB/PBNPs nanocomposite was synthesized according to previous work [12] and used for the preparation of a 0.06 mg/mL dispersion in a mixture of N,N-dimethylformamide and distilled water 1:1 (v/v) as the solvent, followed by sonication for 60 min at 59 kHz.

2.3. Hydrogen peroxide detection in solution

The chronoamperometric technique was used for hydrogen peroxide detection by connecting SPEs to a smartphone-assisted miniaturized potentiostat (Sensit Smart, PalmSens, The Netherlands). Chronoamperometry measurements were performed by dropping 40 μL of standard solution at different concentrations of hydrogen peroxide onto the electrochemical cell and applying a potential of −0.05 V vs Ag/AgCl pseudoreference for 30 s. The obtained current intensity was proportional to the amount of hydrogen peroxide present in the standard solution. All the solutions were prepared in 0.05 M phosphate buffer containing 0.1 M KCl at pH = 7.4.

2.4. Hydrogen peroxide detection in aerosol phase

Hydrogen peroxide detection in the aerosol phase was carried out by directly exposing the SPEs to nebulized solution for 30 s at 0.5 cm from the nebulizer, in order to wet the cellulose network homogeneously. Before the measurement, the sensor is loaded with 5 μL of phosphate buffer at pH = 7.4 and let to dry; then, it is ready for hydrogen peroxide detection in the aerosol phase. Immediately after the accumulation time, the chronoamperometric detection was performed with the same parameters described in paragraph 2.3. The solutions were nebulized by using a commercially available ultrasonic aroma diffuser, with a flow rate equal to 0.6 mL/min.

2.5. Experimental set-up for the evaluation of disinfectant property of the commercial available ultrasonic aroma diffuser loaded with hydrogen peroxide

To evaluate the disinfectant capability of the commercially available ultrasonic aroma diffuser, the settle plate method was selected to evaluate the efficiency of disinfection, counting colony-forming units (CFU) of bacteria naturally present in the air before and after the exposure to the hydrogen peroxide aerosol. The study was carried out using hydrogen peroxide at 5% (w/w) in a room of 63 m^3, positioning the diffuser 1,50 m high in the corner 2 and the settle plates at the 4 corners of the room (1, 2 , 3, 4). The settle plates were located in all the sites before starting the disinfection (blank experiment) and during and after the disinfection lasting 1 h, at different times: T0 (during the disinfection), T1 (at the end of the disinfection for 2 h), T2 (4 h after the disinfection T0), and T3 (6 h after the disinfection T0).

For the blank experiment, the sterile plates with culture medium were exposed to the room air for 2 h. T0 sample was considered when the diffuser was running for 1 h. Then the machine was turned off and settle plate samples were taken every 2 h for 3 times (T1, T2, T3).

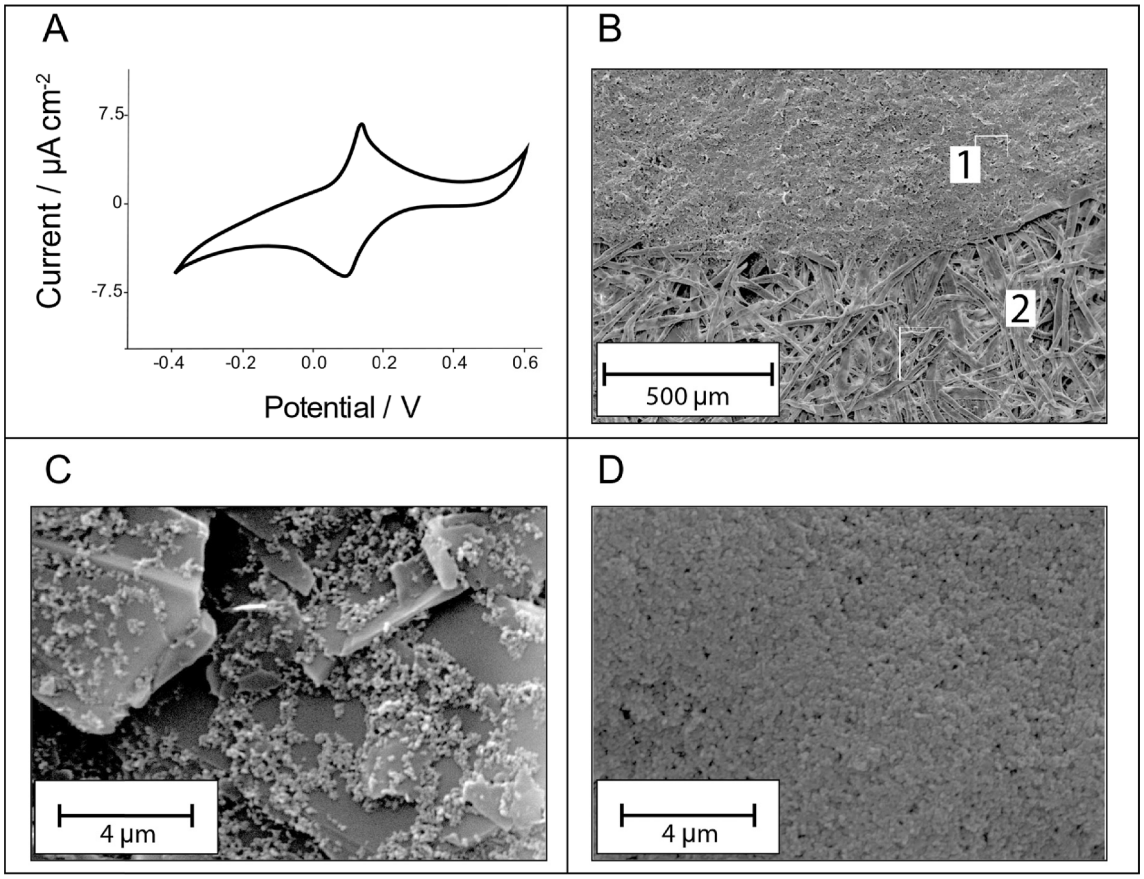

Fig. 1. A) Cyclic voltammetry performed in phosphate buffer 0.05 M + KCl 0.1 M, pH 7.4, using paper-based sensor. B) SEM micrograph of the bare screen-printed electrode depicting graphite-based working electrode (1) and paper substrate (2). C) SEM micrograph of bare screen-printed electrode. D) SEM micrograph of screen-printed electrode modified with carbon black-Prussian Blue nanoparticles.

After every sampling, the plates were closed, incubated at 37 °C for 48 h for bacteria and at 28 °C for 72 h for fungi and the number of CFU was recorded.

3. Results and discussion

3.1. Paper-based sensor for hydrogen peroxide detection in solution

The electrochemical detection of hydrogen peroxide at a screen-printed bare electrode is avoided due to the high overpotential needed. As widely reported in the literature [13], Prussian Blue electrochemical mediator has demonstrated outstanding electrocatalytic activity, being able to electrocatalyze the reduction of hydrogen peroxide to water at potential close to 0 vs Ag/AgCl, the reason for that it was called artificial peroxidase. Recently, we have demonstrated that the presence of carbon black nanomaterial is able to customize the dimension of Prussian Blue nanoparticles during its synthesis. Using carbon black as support, the chemical synthesis with potassium ferricyanide and potassium hexacyanoferrate allowed for obtaining a carbon black decorated with Prussian Blue nanoparticles characterized by a diameter of 19 ± 3 nm and low detection limit, i.e. 0.3 μM for hydrogen peroxide [12]. Using filter paper, we usually modify the ink during the screen-printing process with the powder of carbon black decorated with Prussian Blue nanoparticles, (i.e. bulk modification), because in the case of porous paper, the reaction occurs between the solution entrapped in the layer of the cellulose network and the working electrode surface in contact with the paper (i.e. the backside of the working electrode) [14,15]. On the contrary, in the case of office paper, we modify the working electrode surface by drop-casting the dispersion of carbon black-Prussian Blue nanoparticles; being office paper not so porous, the solution remains on the electrochemical cell as drop [15]. In our previous paper, we demonstrated the suitability of bulk modification also in the case of office paper for the detection of capsaicin [16]. Herein, we evaluated the possibility to use the drop-casting approach also in case of filter paper. Fig. 1A shows the cyclic voltammetry of carbon black-Prussian Blue nanoparticles-modified filter paper-based sensor in phosphate buffer solution at pH = 7.4. The cyclic voltammetry reported a characteristic couple of peaks at a potential close to 0.2 V due to the oxidation and reduction reaction of Prussian Blue nanoparticles as follows:

$$KFe^{III}\left[Fe^{II}(CN)_6\right] + e^- + K^+ \rightleftarrows K_2Fe^{II}\left[Fe^{II}(CN)_6\right]$$

demonstrating the presence of the electrochemical mediator on the working electrode surface. Furthermore, the small distance between peak-to-peak potentials (i.e. 40 mV) as well as the ratio of cathodic and anodic peak currents close to one, remarks the typical behaviour of an electroactive specie adsorbed on the electrode surface. To confirm the presence of the nanocomposite on the working electrode surface, the morphological characterization was carried out by SEM analysis. Fig. 1B-D showed micrographs of screen-printed electrode printed on filter paper and of screen-printed electrode printed on filter paper and modified with carbon black-Prussian Blue nanoparticles dispersion. As depicted in Fig. 1B, the primary fiber structure of the paper is highlighted, covered with a layer of graphite-based ink in the working electrode area. The high magnification micrograph of the bare screen-printed electrode (Fig. 1C) reported micrometer-sized flakes of graphite covered with small particles ascribed to the cross-linking as well nanoparticle-based agents in the original ink. Fig. 1D reported SEM micrograph of the working electrode modified with carbon black-

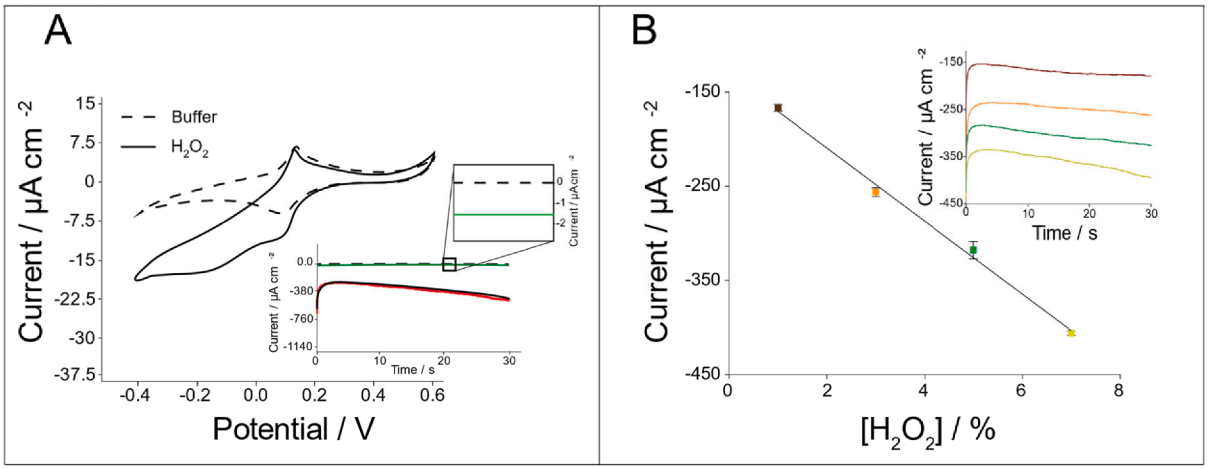

Fig. 2. A) Cyclic voltammetries using sensors printed on filter paper and modified with carbon black-Prussian Blue nanoparticles in absence (dashed line) and in presence (continuous line) of hydrogen peroxide 0.003 % w/w. Inset: Chronoamperograms recorded for hydrogen peroxide detection at a concentration of 7 % w/w, using bare electrode (dashed line), electrode modified with carbon black-Prussian Blue nanoparticles dispersion via drop-casting (black line), electrode bulk modified adding carbon black-Prussian Blue nanoparticle in the ink during the screen-printing procedure (green line), and electrode modified via bulk plus via drop-casting (red line). B) Calibration curve of hydrogen peroxide carried out in phosphate buffer 0.05 M + KCl 0.1 M, pH = 7.4 at an applied potential of −0.05 V vs Ag/AgCl. Inset: chronoamperograms recorded using SPE modified with carbon black-Prussian Blue nanoparticles for hydrogen peroxide detection at a concentration equal to 1% (brown), 3% (orange), 5% (green), 7% (yellow).

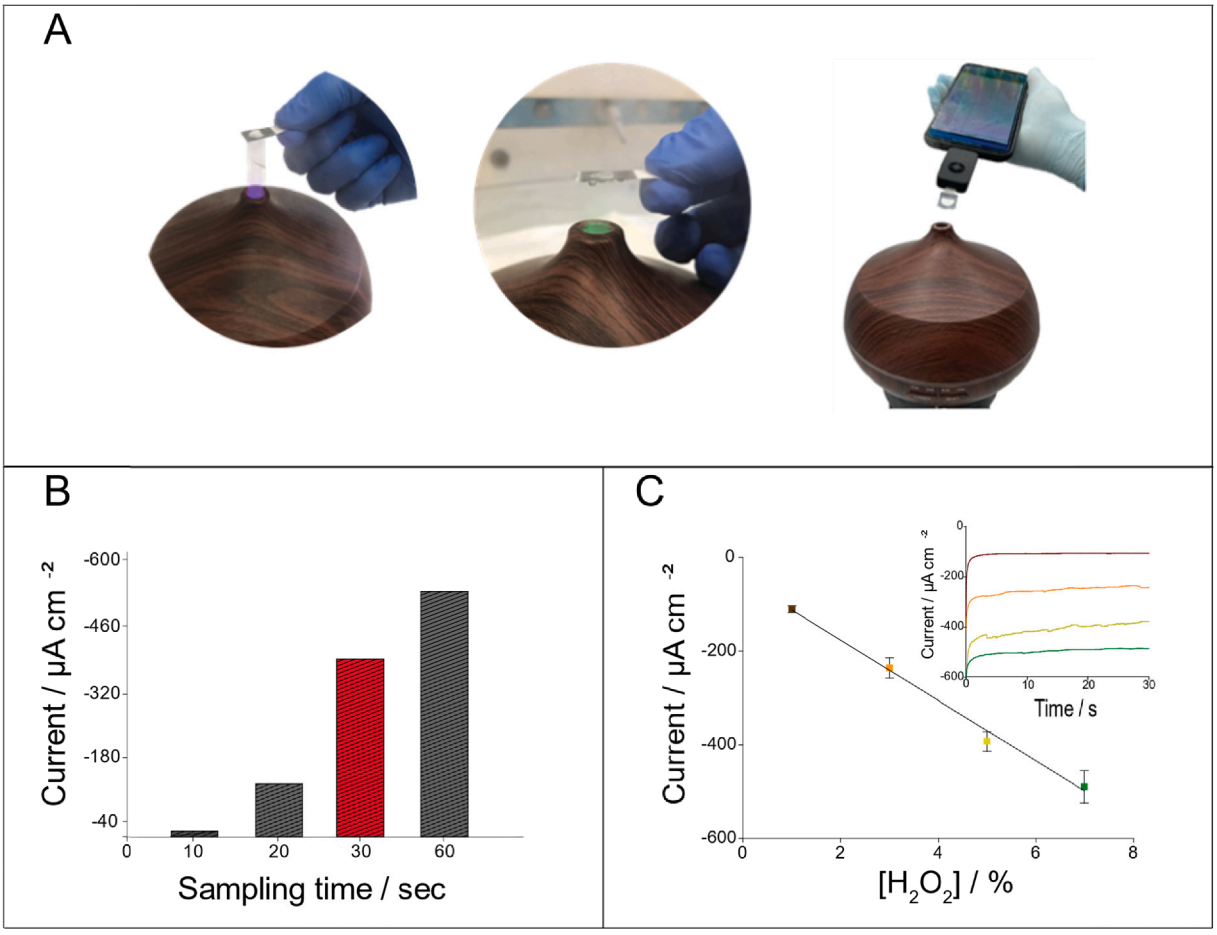

Fig. 3. A) Experimental set-up using the sensor exposed to hydrogen peroxide nebulized during the study of sampling time and the using the embedded system constituted of a sensor combined with smartphone assisted potentiostat. B) Selection of sampling time using a solution of hydrogen peroxide at a concentration of 5% w/w in the ultrasound diffuser. C) Calibration curve sampling the aerosol of hydrogen peroxide at 30 sec at an applied potential of −0.05 V vs Ag/AgCl using the embedded system constituted of a sensor combined with smartphone assisted potentiostat. Inset: Chronoamperograms recorded using SPE modified with carbon black-Prussian Blue nanoparticles for hydrogen peroxide detection at a concentration equal to 1% (brown), 3% (orange), 5% (yellow), 7% (green).

Table 1
Sensors for hydrogen peroxide in aerosol/gas phase.

Sensor types	Detection method	Sensitivity	Linear range	Comments	Ref.
Pt-Nafion	Amperometric	3.3 μA ppm^{-1}	0.1–40 ppm	Bulk electrodes, No flexible and cost-effective sensor, Low detection limit	[17]
Thin-film calorimetric sensor	Calorimetric	0.57 °C/% (v/v) (51 × 10^{-6} °C ppm^{-1})	0–8% v/v (0–89 × 10^3 ppm)	High working temperature (270 °C) No flexible and cost-effective sensor Detection of high concentrations	[18]
Paper-based wearable electrochemical sensor	Amperometric	0.02 nA μM^{-1} mm^{-2} (0.59 nA ppm^{-1} mm^{-2})	40–320 μM (1.36–10.88 ppm)	Flexible and cost-effective sensor Low detection limit Chromatography paper and screen-printed electrode using Prussian Blue modified ink Application in biomedical field	[11]
Commercial H_2O_2 gas sensor	–	–	0–100 ppm 100–2000 ppm	No flexible and cost-effective sensor	[19]
MOSFET	Output voltage	–	Detection limit close to 0.8 μM (0.027 ppm)	Hydrogen peroxide is measured in the condensed phase using Peltier element No flexible and cost-effective sensor	[20]
Paper-based electrochemical sensor	Amperometric	64 μA/% (w/w) cm^2 (5.8 × 10^{-3} μA ppm^{-1} cm^{-2})	1–7% w/w (11–78 × 10^3 ppm)	Filter paper and screen-printed electrode modified *via* drop-casting with carbon black/Prussian Blue nanoparticles Flexible and cost-effective sensor	This work

Prussian Blue nanoparticles which underlined the rough and sponge-like structure of carbon black-Prussian Blue nanocomposite, confirming the presence of the electrochemical mediator onto the working electrode surface.

To evaluate the effectiveness of the paper-based electrode modified with carbon black-Prussian Blue nanoparticle dispersion for the detection of hydrogen peroxide, cyclic voltammetry in absence (dashed line) and in presence (continuous line) of hydrogen peroxide 0.003% w/w was carried out and reported in Fig. 2A. The measure was carried out by adding 40 μL of phosphate buffer solution at pH = 7.4 on the electrochemical cell without or with hydrogen peroxide. The cyclic voltammetry in presence of hydrogen peroxide has shown an increase of the cathodic peak and a decrease of the anodic peak, when compared with the cyclic voltammetry in absence of hydrogen peroxide, confirming the electrocatalytic activity of the carbon black-Prussian Blue nanoparticles towards hydrogen peroxide reduction. In the inset, we report the amperometric responses of hydrogen peroxide at a concentration of 7% w/w, using the three different configurations, namely SPE modified with the dispersion *via* drop-casting (black line), SPE bulk modified adding carbon black-Prussian Blue nanoparticle in the ink during the screen-printing procedure (green line), and SPE modified *via* bulk plus *via* drop-casting (red line). The amperograms depicted the same response, within the experimental errors, in case of SPE modified *via* drop-casting or bulk plus *via* drop-casting, in contrast with a lower sensitivity observed in case of the single bulk modification. Thus, the paper-based sensor modified *via* drop-casting was selected for further studies. Successively, we evaluated the analytical performances in chronoamperometry by checking the sensitivity of the sensor, obtaining a linear range suitable for the concentration necessary for the disinfection process, namely 1–7% w/w. Indeed, this sensor is able to detect several ranges of hydrogen peroxide concentration; for instance between 0.003 and 0.03% w/w the linear range is described by the following equation $y = (-8 \pm 4) + (-49 \pm 1) \times$, $R^2 = 0.996$. However, we focalized the detection of hydrogen peroxide at concentrations used for disinfection (between 1% and 7% w/w). As reported in Fig. 2B, the sensor is able to detect hydrogen peroxide comprised between 1% and 7% w/w, described by the following equation: $y = (-132 \pm 6) + (-38 \pm 1) \times$, $R^2 = 0.991$. The repeatability was evaluated by testing a concentration of hydrogen peroxide at a concentration of 7% w/w with three different sensors and obtaining an RSD % equal to 1%.

3.2. Paper-based sensor for hydrogen peroxide detection in aerosol phase

For the hydrogen peroxide detection in the aerosol phase, the sensor was put in proximity of the aerosol as reported in Fig. 3A. The first study was the evaluation of the time of exposure to the aerosol, because this time is needed to wet the cellulose network of the sensor and to enrich it with the hydrogen peroxide. It is worthy of note that for delivering a reagent-free sensor, the sensor is loaded with phosphate buffer at pH = 7.4, then left to dry. Thus, when the aerosol wet the sensor, the film of the solution formed in the cellulose network is at pH = 7.4, because dissolving the phosphate buffer salts previously loaded on the paper. As reported in Fig. 3B, the time selected was 30 sec as a compromise between sensitivity and wetting process, while a longer time allowed wetting also the electric contacts with an incorrect electronic measure. After selecting the time, the calibration curve was evaluated using different concentrations of hydrogen peroxide in the ultrasound diffuser, obtaining a linear range up to 7% w/w, described by the following equation: $y = (-48 \pm 14) + (-64 \pm 3) \times$, $R^2 = 0.978$, and a repeatability with RSD = 7% (n = 3) testing a solution of hydrogen peroxide equal to 7% w/w. The results achieved demonstrate the suitability of this sensor for evaluating the nebulized hydrogen peroxide, with the advantages, with respect to the sensors reported in the literature (Table 1), to detect high concentration level needed for disinfection as well as to be a cost-effective and flexible paper-based sensor combined with a smart-phone assisted potentiostat.

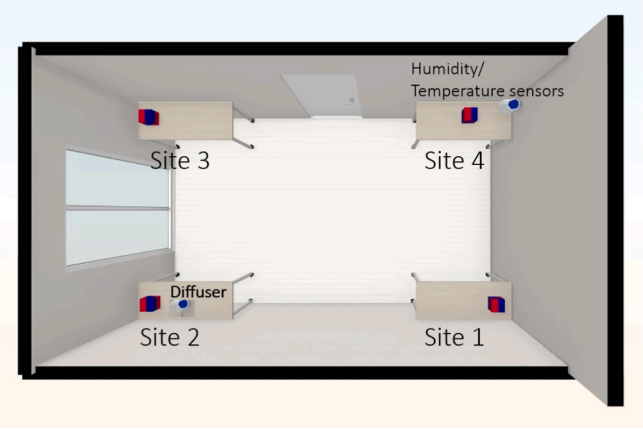

Fig. 4. Room planimetry.

Table 2
Bacterial and fungal counts in the room.

Sampling Time	Sampling Period	Temperature	Humidity	Site 1		Site 2		Site 3		Site 4	
				Fungi	Bacteria	Fungi	Bacteria	Fungi	Bacteria	Fungi	Bacteria
Blank	2 h	20.3 °C	62%	22 CFU	92 CFU	13 CFU	52 CFU	11 CFU	50 CFU	29 CFU	54 CFU
T0 (vapour dispersal)	1 h	20.4 °C	62%	12 CFU	54 CFU	10 CFU	16 CFU	7 CFU	22 CFU	5 CFU	10 CFU
T1	2 h	20.4 °C	62%	15 CFU	12 CFU	11 CFU	19 CFU	9 CFU	9 CFU	6 CFU	11 CFU
T2	2 h	20.4 °C	62%	16 CFU	14 CFU	14 CFU	14 CFU	19 CFU	10 CFU	19 CFU	18 CFU
T3	2 h	20.4 °C	62%	17 CFU	17 CFU	13 CFU	20 CFU	22 CFU	14 CFU	22 CFU	36 CFU

3.3. Test to assess the disinfection process using an ultrasonic diffuser and hydrogen peroxide at a concentration of 5% w/w

To confirm the utility of the sensor developed to assess the presence of hydrogen peroxide vaporized by an ultrasonic diffuser, we evaluated the antimicrobial activity of hydrogen peroxide 5% w/w vaporized by ultrasonic diffuser on airborne bacteria and fungi.

The adopted hydrogen peroxide concentration was selected in order to have a good compromise between solution stability and disinfection performance. In fact, hydrogen peroxide solutions with concentrations higher than 10% w/w are usually unstable over time and can be corrosive and potentially explosive. On the other hand, 3% w/w hydrogen peroxide solution would require very high volumes to obtain acceptable disinfection.

The experiment was performed in a room of 63 m^3, where the door and window remained closed during the experiment. The diffuser was placed as shown in Fig. 4, while the blue/red boxes indicated the position of the settle plates.

The first set of plates was placed for two hours in the room before starting the disinfection to evaluate the pre-existing microbial presence in the room (blank experiment). Then, the plates were displaced with new ones and the disinfection was carried out for 1 h by switching-on the diffuser. After disinfection, the microbiological efficiency of the treatment was evaluated every 2 h for 6 h by counting bacterial and fungal visible colonies grown on the plates. The results obtained were reported in Table 2.

Results showed a fast and strong decrease in the bacterial load in the room. In particular, during the supply of the disinfectant solution in the air, a sharp decrease of the CFU was detected, in the range comprised between around 40% and 80% depending on the initial amount of bacteria and the site of the plates with respect to the diffuser. We would like to highlight that this system was used in a room without any additional source of contamination. Under this experimental condition, we demonstrated the effect of disinfection as well as that the developed sensor is capable to measure the level of hydrogen peroxide needed for this disinfection process.

4. Conclusions

In the last decade, paper-based electrochemical sensors have demonstrated the potentiality to be used in diverse contexts, ranging from point of care devices through wearable sensors for the detection of analytes in liquidand gas-phase [21,22]. Herein, we reported the use of a filter paper-based electrochemical device for the detection of hydrogen peroxide nebulized by using a cost-effective ultrasonic aroma reconverted diffuser. By modifying the filter paper-based sensor *via* drop-casting, we demonstrated that this procedure is not only applicable to office paper-based sensors but also to filter paper-based sensors, enlarging the applicability of this easy mass-modification procedure. The sensor developed was tested using hydrogen peroxide solution in a concentration ranging from 1% to 7% w/w, demonstrating linearity in the analyzed range corresponding to the concentrations usually employed for disinfection processes. The data reported in this short communication demonstrated the capability of paper-based electrochemical sensors to detect the nebulized hydrogen peroxide, paving the way for its use in the customization of the disinfection processes.

CRediT authorship contribution statement

Luca Fiore: Investigation, Methodology, Writing - review & editing. **Vincenzo Mazzaracchio:** Methodology, Writing - review & editing. **Pierluca Galloni:** Conceptualization, Methodology, Writing - review & editing. **Federica Sabuzi:** . **Silvia Pezzola:** . **Giorgia Matteucci:** Investigation, Methodology, Writing - review & editing. **Danila Moscone:** Writing - review & editing. **Fabiana Arduini:** Conceptualization, Methodology, Writing - review & editing.

Declaration of Competing Interest

The authors declare that they have no known competing financial interests or personal relationships that could have appeared to influence the work reported in this paper.

Acknowledgements

Authors thank Prof. Letizia Di Bella and Dr. Marco Albano (Laboratorio di Microscopia Elettronica e Microanalisi del Dipartimento di Scienze delle Terra, Università di Roma la Sapienza) for SEM analysis.

References

[1] Scientific Brief: SARS-CoV-2 and Potential Airborne Transmission. https://www.cdc.gov/coronavirus/2019-ncov/more/scientific-brief-sars-cov-2.html, 2020 (accessed 26 November 2020).
[2] L. Bourouiba, Turbulent gas clouds and respiratory pathogen emissions: potential implications for reducing transmission of COVID-19, JAMA (2020), https://doi.org/10.1001/jama.2020.4756.
[3] A.W.H. Chin, J.T.S. Chu, M.R.A. Perera, K.P.Y. Hui, H.-L. Yen, M.C.W. Chan, M. Peiris, L.L.M. Poon, Stability of SARS-CoV-2 in different environmental conditions, Lancet Microbe 1 (2020), e10, https://doi.org/10.1016/S2666-5247(20)30003-3.
[4] Cleaning and disinfection of environmental surfaces in the context of COVID-19. https://www.who.int/publications/i/item/cleaning-and-disinfection-of-environmental-surfaces-inthe-context-of-covid-19, 2020 (accessed 26 November 2020).
[5] D.J. Weber, W.A. Rutala, D.J. Anderson, L.F. Chen, E.E. Sickbert-Bennett, J. M. Boyce, Effectiveness of ultraviolet devices and hydrogen peroxide systems for terminal room decontamination: Focus on clinical trials, Am. J. Infect. Control. 44 (2016) e77–e84, https://doi.org/10.1016/j.ajic.2015.11.015.
[6] F. Arduini, D. Moscone, Multifarious aspects of electrochemical paper-based (bio) sensors, Compr. Anal. Chem. Elsevier (2020) 139–161, https://doi.org/10.1016/bs.coac.2020.01.001.
[7] A. Antonacci, V. Scognamiglio, V. Mazzaracchio, V. Caratelli, L. Fiore, D. Moscone, F. Arduini, Paper-based electrochemical devices for the pharmaceutical field: state of the art and perspectives, Front. Bioeng. Biotechnol. 8 (2020) 339, https://doi.org/10.3389/fbioe.2020.00339.
[8] F. Arduini, S. Cinti, V. Caratelli, L. Amendola, G. Palleschi, D. Moscone, Origami multiple paper-based electrochemical biosensors for pesticide detection, Biosens. Bioelectron. 126 (2019) 346–354, https://doi.org/10.1016/j.bios.2018.10.014.
[9] V. Caratelli, A. Ciampaglia, J. Guiducci, G. Sancesario, D. Moscone, F. Arduini, Precision medicine in Alzheimer's disease: An origami paper-based electrochemical device for cholinesterase inhibitors, Biosens. Bioelectron. 165 (2020), 112411, https://doi.org/10.1016/j.bios.2020.112411.
[10] N. Colozza, K. Kehe, G. Dionisi, T. Popp, A. Tsoutsoulopoulos, D. Steinritz, D. Moscone, F. Arduini, A wearable origami-like paper-based electrochemical

biosensor for sulfur mustard detection, Biosens. Bioelectron. 129 (2019) 15–23, https://doi.org/10.1016/j.bios.2019.01.002.
[11] D. Maier, E. Laubender, A. Basavanna, S. Schumann, F. Güder, G.A. Urban, C. Dincer, Toward continuous monitoring of breath biochemistry: A paper-based wearable sensor for real-time hydrogen peroxide measurement in simulated breath, ACS Sens. 4 (2019) 2945–2951, https://doi.org/10.1021/acssensors.9b01403.
[12] S. Cinti, F. Arduini, G. Vellucci, I. Cacciotti, F. Nanni, D. Moscone, Carbon black assisted tailoring of Prussian Blue nanoparticles to tune sensitivity and detection limit towards H_2O_2 by using screen-printed electrode, Electrochem. Commun. 47 (2014) 63–66, https://doi.org/10.1016/j.elecom.2014.07.018.
[13] F. Ricci, G. Palleschi, Sensor and biosensor preparation, optimisation and applications of Prussian Blue modified electrodes, Biosens. Bioelectron. 21 (3) (2005) 389–407, https://doi.org/10.1016/j.bios.2004.12.001.
[14] G. Scordo, D. Moscone, G. Palleschi, F. Arduini, A reagent-free paper-based sensor embedded in a 3D printing device for cholinesterase activity measurement in serum, Sensor. Actuat. B Chem. 258 (2018) 1015–1021, https://doi.org/10.1016/j.snb.2017.11.134.
[15] S. Cinti, D. Moscone, F. Arduini, Preparation of paper-based devices for reagentless electrochemical (bio)sensor strips, Nat. Protoc. 14 (8) (2019) 2437–2451, https://doi.org/10.1038/s41596-019-0186-y.
[16] P.B. Deroco, O. Fatibello-Filho, F. Arduini, D. Moscone, Electrochemical determination of capsaicin in pepper samples using sustainable paper-based screen-printed bulk modified with carbon black, Electrochim. Acta 354 (2020), 136628, https://doi.org/10.1016/j.electacta.2020.136628.
[17] R. Toniolo, P. Geatti, G. Bontempelli, G. Schiavon, Amperometric monitoring of hydrogen peroxide in workplace atmospheres by electrodes supported on ion-exchange membranes, J. Electroanal. Chem. 514 (1-2) (2001) 123–128, https://doi.org/10.1016/S0022-0728(01)00612-X.
[18] P. Kirchner, B. Li, H. Spelthahn, H. Henkel, A. Schneider, P. Friedrich, J. Kolstad, M. Keusgen, M.J. Schöning, Thin-film calorimetric H2O2 gas sensor for the validation of germicidal effectivity in aseptic filling processes, Sensor. Actuat. B Chem. 154 (2) (2011) 257–263, https://doi.org/10.1016/j.snb.2010.01.058.
[19] https://en.gazdetect.com/catalog/fixed-H2O2-hydrogen-peroxide-detector-b12/.
[20] D.T.V. Anh, W. Olthuis, P. Bergveld, A hydrogen peroxide sensor for exhaled breath measurement, Sens. Actuat. B Chem. 111–112 (2005) 494–499, https://doi.org/10.1016/j.snb.2005.03.107.
[21] S. Khan, S. Ali, A. Bermak, Recent developments in printing flexible and wearable sensing electronics for healthcare applications, Sensors 19 (2019) 1230, https://doi.org/10.3390/s19051230.
[22] E.W. Nery, L.T. Kubota, Sensing approaches on paper-based devices: a review, Anal. Bioanal. Chem. 405 (2013) 7573–7595, https://doi.org/10.1007/s00216-013-6911-4.